

See discussions, stats, and author profiles for this publication at: <https://www.researchgate.net/publication/51214197>

Silver Bioaccumulation Dynamics in a Freshwater Invertebrate after Aqueous and Dietary Exposures to Nanosized and Ionic Ag

ARTICLE in ENVIRONMENTAL SCIENCE & TECHNOLOGY · JUNE 2011

Impact Factor: 5.33 · DOI: 10.1021/es200880c · Source: PubMed

CITATIONS

72

READS

123

4 AUTHORS:



Marie Noele Croteau

United States Geological Survey

33 PUBLICATIONS 837 CITATIONS

SEE PROFILE



Superb K Misra

University of Birmingham

45 PUBLICATIONS 1,278 CITATIONS

SEE PROFILE



Samuel N Luoma

University of California, Davis

211 PUBLICATIONS 10,485 CITATIONS

SEE PROFILE



Eva Valsami-Jones

University of Birmingham

57 PUBLICATIONS 1,054 CITATIONS

SEE PROFILE

Silver Bioaccumulation Dynamics in a Freshwater Invertebrate after Aqueous and Dietary Exposures to Nanosized and Ionic Ag

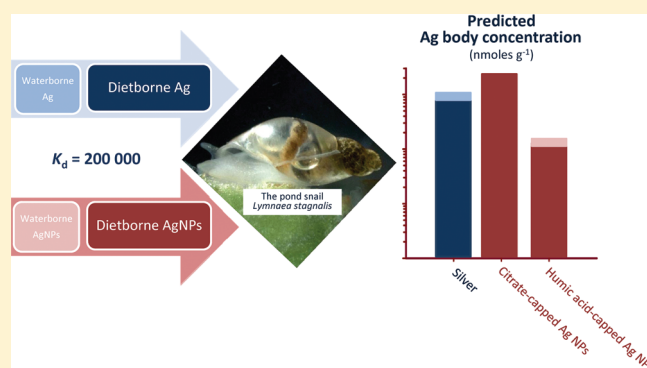
Marie-Noëlle Croteau,^{†,*} Superb K. Misra,[‡] Samuel N. Luoma,^{†,‡} and Eugenia Valsami-Jones[‡]

[†]U.S. Geological Survey, 345 Middlefield Road Menlo Park, California 94025, United States

[‡]Department of Mineralogy, Natural History Museum, Cromwell Road, London, SW7 5BD, United Kingdom

 Supporting Information

ABSTRACT: We compared silver (Ag) bioavailability and toxicity to a freshwater gastropod after exposure to ionic silver (Ag⁺) and to Ag nanoparticles (Ag NPs) capped with citrate or with humic acid. Silver form, exposure route, and capping agent influence Ag bioaccumulation dynamics in *Lymnaea stagnalis*. Snails efficiently accumulated Ag from all forms after either aqueous or dietary exposure. For both exposure routes, uptake rates were faster for Ag⁺ than for Ag NPs. Snails efficiently assimilated Ag from Ag NPs mixed with diatoms (assimilation efficiency (AE) ranged from 49 to 58%) and from diatoms pre-exposed to Ag⁺ (AE of 73%). In the diet, Ag NPs damaged digestion. Snails ate less and inefficiently processed the ingested food, which adversely impacted their growth. Loss rates of Ag were faster after waterborne exposure to Ag NPs than after exposure to dissolved Ag⁺. Once Ag was taken up from diet, whether from Ag⁺ or Ag NPs, Ag was lost extremely slowly. Large Ag body concentrations are thus expected in *L. stagnalis* after dietborne exposures, especially to citrate-capped Ag NPs. Ingestion of Ag associated with particulate materials appears as the most important vector of uptake. Nanosilver exposure from food might trigger important environmental risks.



INTRODUCTION

The environmental risk of silver nanoparticles (Ag NPs) is a current and highly topical focus of concern. Silver antibacterial properties are being exploited in a rapidly growing range of consumer goods.¹ Release of Ag into the environment from this emerging nanotechnology is inevitable (e.g., ref 2). Yet, very little is known about the environmental fate, bioavailability and effects of exposure to Ag NPs.

Ionic silver (Ag⁺) is extremely toxic to bacteria.³ It also adversely affects phytoplankton, invertebrates, and fish.⁴ At the nanosized scale, Ag can be toxic at very low concentrations. After exposures ranging from 0.04 to 0.71 nM, Lee et al.⁵ showed that citrate-capped Ag NPs are transported inside developing zebra fish embryos, eliciting deformities and causing death.

Bioavailability is important in determining toxicity. Bioavailability can be defined by the ability of a metal species to associate with a cell membrane and be internalized. Mechanistically, this translates into a metal concentration taken up by an organism from all possible uptake pathways, including water and food.⁶ The dynamics of uptake and loss (i.e., bioaccumulation dynamics, or biodynamics) can influence toxicity.⁷ Therefore, knowledge of biodynamics is a prerequisite for understanding and evaluating toxicity. However, much remains to be learned about the mechanisms controlling the biodynamics and toxicity of Ag NPs.

It is unclear whether (or when) Ag NPs toxicity is caused by the nanoparticle itself or its release of Ag ions by solubilization.^{8,9} For example, Navarro et al.¹⁰ showed that Ag NPs enhanced toxicity by providing a source of Ag⁺ to green algae. Garcia-Alonso et al.,¹¹ in contrast, showed that Ag NPs were taken up into the gut tissues of polychaetes when animals were exposed to the Ag NPs via their food. If nanoparticles are bioaccumulated, however, then it might be expected that their biodynamics would differ from those of Ag⁺.

Capping agents are commonly employed to modify the surface of nanoparticles, but their influence on bioavailability and toxicity is not well studied. In addition to influencing the release of Ag⁺ from Ag NPs,¹² surface coatings might facilitate the entry of Ag NPs into cells, where they could deliver bioavailable and potentially toxic Ag⁺ (i.e., Trojan horse mechanism¹³). For instance, nanoparticles coated with citrate could conceivably be cotransported on sites specific to citrate.¹⁴ Citrate forms complexes with metals that are bioavailable to aquatic organisms from solution.^{15,16} Humic acids can also form metal-complexes that affect bioavailability of metals^{17,18} and perhaps that of Ag NPs.¹⁹

Received: March 16, 2011

Accepted: June 13, 2011

Revised: June 7, 2011

Published: June 13, 2011

Furthermore, the change in surface chemistry caused by capping agents could influence uptake pathways, favoring either waterborne uptake (by preventing particle aggregation and increasing their persistence in solution), or dietary uptake (if the particles aggregate and sediment).

In addition to factors intrinsic to nanoparticles (e.g., size, shape and surface chemistry), physiological processes can influence the inward and outward fluxes of metal-laden particles in organisms.⁶ But rates of uptake and loss of nanosized metals are rarely quantified. Here we develop rates of uptake and loss for Ag⁺ and Ag NPs and use these to model Ag biodynamics between Ag forms and exposure routes. We ask, what is the major uptake pathway of Ag NPs? How do rates of uptake and loss of Ag NPs compare with those for Ag⁺? How do capping agents affect bioavailability and toxicity? We also test whether Ag elicit adverse responses in the gut, or in the whole organism.

METHODS

Silver Nanoparticles. Silver nanoparticles were synthesized as described in Misra et al.⁹ (Figure S1 of the Supporting Information, SI). The citrate capped Ag NPs (cit-Ag NPs) had an average TEM size of 17 ± 5 nm ($n = 200$) and a ζ potential of -28.2 ± 0.7 mV in moderately hard water (MOD, Table S1 of the SI). The humic acid capped Ag NPs (HA-Ag NPs) were 13 ± 3 nm in size ($n = 200$) and had a ζ potential of -35 ± 2 mV in MOD water. Both Ag NPs formed monodispersed suspensions in MOD.

The Biodynamic Model. Biodynamic modeling deconstructs metal bioaccumulation and quantifies its mechanistic components. As shown in eq 1, metal influx from solution is expressed as a function of k_{uw} ($l\ g^{-1}\ d^{-1}$), a unidirectional metal uptake rate constant from solution, and the dissolved or dispersed metal concentrations ($[M]_{water}$, nmol l^{-1}). Metal influx from food varies as a function of k_{uf} ($g\ g^{-1}\ d^{-1}$), a unidirectional metal uptake rate constant from food, and the dietborne metal concentrations ($[M]_{food}$, nmol g^{-1}). The rate constant k_{uf} can be expressed as a function of food ingestion rate (IR, $g\ g^{-1}\ d^{-1}$) and metal assimilation efficiency (AE, unit less) (eqs S1–S4 of the SI). Metal effluxes vary as a function of the rate constant for physiological loss (k_e , d^{-1}), the rate constant for body growth dilution (k_g , d^{-1}), and the metal concentration in the organism ($[M]_{organism}$, nmol g^{-1}) (eq S5).

$$[M]_{organism} = \underbrace{k_{uw} \times [M]_{water}}_{\text{waterborne uptake}} + \underbrace{k_{uf} \times [M]_{food}}_{\text{dietborne uptake}} - \underbrace{k_e \times [M]_{organism}}_{\text{elimination}} - \underbrace{k_g \times [M]_{organism}}_{\text{body growth dilution}} \quad (1)$$

Membrane Transport Characteristics. Metal influx ($\text{Influx}_{organism}$, nmol $g^{-1}\ d^{-1}$) can also be interpreted mechanistically as the result of processes that characterize membrane transport,

$$\text{Influx}_{organism} = \frac{B_{max} [M]_{exposure}}{K_{metal} + [M]_{exposure}} \quad (2)$$

where B_{max} (nmol g^{-1}) represents the number of transport sites, $[M]_{exposure}$ is the metal exposure concentration (nmol l^{-1} or nmol g^{-1}), and K_{metal} (nmol l^{-1} or nmol g^{-1}) represents the affinity of each transport site for a metal.

Experimental Organisms. Freshwater snails (*Lymnaea stagnalis*) were reared in the laboratory in MOD water. Three days prior to each experiment, snails of a restricted size range (mean soft tissue

dry weight of 8.6 ± 0.3 mg 95% CI, $n = 843$) were transferred to a 10 L glass aquarium filled with MOD water. Food was withheld during this period.

Background Ag concentration in each experimental snail was estimated using the slope and y-intercept for the linear relationship between Ag burden in 70 unexposed snails and their dry weight. Using this relationship, Ag background was subtracted from measured Ag concentration for each experimental organism.

Waterborne Uptake Experiments. To characterize Ag uptake from water and to compare k_{uw} for Ag⁺ and Ag NPs, 10 snails were transferred to acid-washed 1 L HDPE containers filled with MOD water spiked with different concentrations of either Ag⁺ (added as AgNO₃, Ultra Scientific), HA-Ag NPs, or cit-Ag NPs (1 container per concentration). Silver exposure concentrations (averaged measurements taken at the beginning and at the end of the experiment) ranged from 0.4 to 60 nM for Ag⁺, from 0.6 to 87 nM for HA-Ag NPs and from 1 to 72 nM for cit-Ag NPs. Speciation modeling using PHREEQC²⁰ indicated that 89% of the total Ag added as AgNO₃ occurred as Ag⁺. The exposure concentrations cover most of the range that might be expected in contaminated waters, i.e., from less than 0.05 nM in pristine waters to 3 nM in urban effluents, although Ag concentrations as high as 330 nM were reported in the effluent of a photographic facility.²¹

Snails were not fed during the 24 h exposure period to minimize fecal scavenging. The exposure was short enough to estimate unidirectional influx but long enough to ensure sufficient Ag accumulation for accurate detection. After exposure, snails were removed from the experimental media, rinsed in ultrapure water and frozen. Before and after the exposure, water samples (2 mL, $n = 3$) were taken from each vial, and acidified with concentrated nitric acid (Baker Ultrex II grade, 2% final concentration).

Dietborne Uptake Experiments. To characterize Ag uptake rates from diet that might be typical of nature and to compare k_{uf} s for Ag⁺ and Ag NPs, we used algae (the benthic diatom *Nitzschia palea*) as a food source. Diatoms were grown axenically for several generations in an S-diatom medium.²² They were harvested onto 1.2- μ m Isopore membrane filters (Millipore) and rinsed with soft water (SO, hardness of 40–48 mg of CaCO₃ L^{-1} ; pH 7.6)²³ to make algal mats.

We first characterized dietborne uptake of Ag⁺ taken up by algae after exposures to Ag in MOD water. We employed the protocol described by Croteau et al.²⁴ to present the algae in a form the snails would ingest, and to ensure that most Ag would be incorporated rather than adsorbed onto the diatoms (Figure S2 of the SI). Briefly, algae were resuspended into a 20 mL acid-washed glass scintillation vial filled with SO water spiked with different concentrations (1 to 500 nM) of a commercially purchased standard of AgNO₃ for 24 h. The pH of the exposure media varied between 6.7 and 7.0. After exposure, diatoms were harvested onto a 1.2- μ m Isopore membrane filter and rinsed with SO water. Small sections of the filters holding the diatoms were sampled and dried for 24 h at 40 °C prior to metal analysis. Silver concentrations in the diatoms varied from 4 to 225 nmoles g^{-1} , which encompass Ag concentrations that can be found in sediments in nature, i.e., from less than a few nmoles g^{-1} in pristine environments to up to 100 nmoles g^{-1} in contaminated systems.¹³

We then characterized the uptake of Ag from Ag NPs mixed with a natural food source, i.e., the diatom *N. palea*. The exposure concentrations ranged from 17 to 187 nmoles g^{-1} for HA-Ag

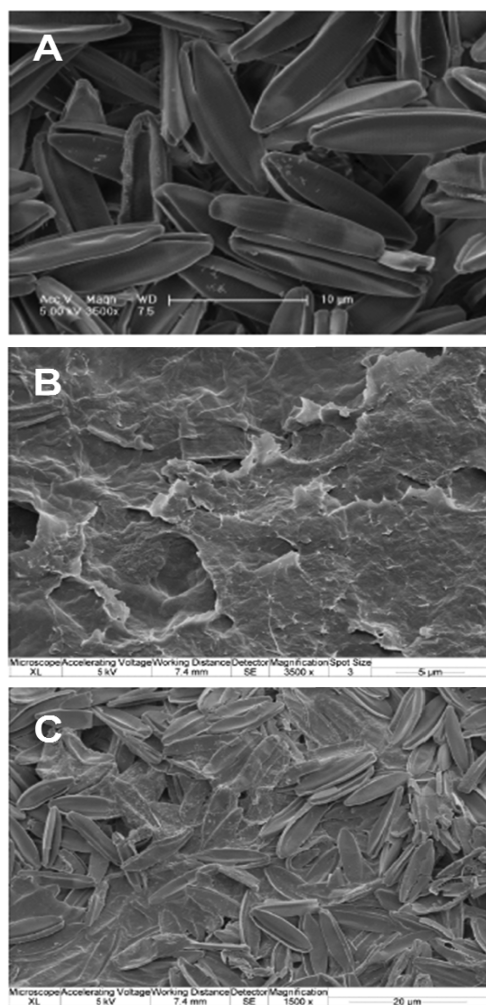


Figure 1. SEM images of (a) diatom mat onto which a low concentration of HA-Ag NPs (17 nmol g^{-1} of Ag as HA-Ag NPs) was filtered through; (b) feces collected after 48 h of depuration for the lowest (17 nmol g^{-1}) and highest (187 nmol g^{-1}) exposure concentrations to HA-Ag NPs.

NPs and from 7 to 250 nmoles g^{-1} for cit-Ag NPs. To achieve these concentrations, we serially diluted suspensions of Ag NPs which were poured onto algal mats and filtered through under low vacuum ($<10 \text{ mm Hg}$) to deposit particles (Figure 1A and Figures S3–S4 of the SI). Small sections of the filters holding the diatoms ($n = 5$) amended with Ag NPs were sampled and dried for 24 h at 40°C prior to imaging and metal analysis.

At each concentration in each treatment, 10 acclimated snails were exposed to the food for 2–4 h. Exposure to the spiked food was shorter than gut residence time,²⁵ which minimizes the confounding influences of efflux and silver recycling. Similar-sized snails were transferred to a 150-mL acid-washed polypropylene vial that was partially submerged in a 40-L glass tank filled with 20-L of MOD water. The animals were allowed to ingest a mass of spiked food (bolus), then removed, rinsed with MOD water, placed individually in acid-washed enclosures and fed uncontaminated food (lettuce) ad libitum for 48 h. The silver retained after complete gut clearance defined “assimilation”.²⁵ After this depuration period, snails were removed from enclosures and frozen. Feces produced by each snail were collected, placed on a piece of acid-washed Teflon sheeting and dried for

24 h at 40°C for imaging and metal analysis. Aliquots of water ($n = 3$) were taken immediately after feeding, as well as at the beginning and the end of depuration. Water samples were acidified with concentrated nitric acid.

Elimination Experiments. To quantify and compare unidirectional efflux rate constants among Ag forms as well as between Ag NPs and exposure routes, we determined loss rate constants after waterborne (k_{ew}) and dietborne exposures (k_{ef}). Ag-specific k_{ew} were determined after exposing snails in MOD water to either $1 \mu\text{g l}^{-1}$ of Ag (from AgNO_3) for 6 days, $10 \mu\text{g l}^{-1}$ of cit-Ag NPs for 1 day, or $50 \mu\text{g l}^{-1}$ of HA-Ag NPs for 1 day in an acid-washed HDPE containers. Snails were not fed during the exposure period to minimize fecal scavenging. To determine Ag-specific k_{ef} , snails were fed for 3–4 h diatoms either pre-exposed to AgNO_3 or mixed with Ag NPs. Specifically, snails were placed in 150 mL acid-washed low-density polyethylene vial partially submerged in a 20 L glass tank filled with MOD water. Filters holding diatoms pre-exposed for 24 h to $50 \mu\text{g L}^{-1}$ of Ag (added as AgNO_3) or amended with either 150 ng of cit-Ag NPs or 500 ng of HA-Ag NPs were placed in vials (Figure S4 of the SI). The different exposure concentrations were necessary to ensure that a sufficiently high initial body concentration of Ag was bioaccumulated from forms of different bioavailability.

After each loading phase, snails were placed into 150-mL acid-washed low-density polyethylene vials partially submerged in a glass tank filled with 20 L of MOD. Snails were fed unlabeled food for up to 25 days while loss of the incorporated Ag occurred. Fecal material was removed from each depuration chamber prior to adding fresh food every 2–3 days. Aliquots of water ($n = 3$) were taken throughout depuration and acidified with concentrated nitric acid. Ten snails were sampled at different time intervals and frozen.

Sample Preparation and Analysis. To minimize inadvertent metal contamination, labware, vials, and Teflon sheeting were soaked for at least 24 h in acid (15% nitric and 5% hydrochloric), rinsed several times in ultrapure water and dried under a laminar-flow hood prior to use.

Partially thawed *L. stagnalis* were dissected to remove soft tissue, placed individually on a piece of acid-washed Teflon sheeting and allowed to dry at 40°C for 3 days. Dried snails, feces and diatoms were weighed and digested in concentrated nitric acid and hydrogen peroxide (Baker Ultrex II grade), following the protocol described in Croteau et al.²⁴ Similar weight samples of the certified reference material NIST-2976 (mussel tissue from National Institute of Standards and Technology) were submitted to the same digestion procedure during each analytical run. Water and digested samples were analyzed for Ag by inductively coupled plasma-mass spectrometry (ICP-MS, SI).

RESULTS

Silver Uptake from Solution. Silver uptake rates increase with concentration through the lower range of exposures for all forms of Ag (Figure 2A–C), although snail Ag background concentration ($\sim 1.3 \text{ nmol g}^{-1}$) impeded detecting Ag accumulation in these short exposures (Figure S5A of the SI) at concentrations below 2 nmol l^{-1} . The uptake rate constants from water ($k_{\text{uw}} \pm 95\% \text{ C.I. in } \text{l g}^{-1} \text{ d}^{-1}$), as determined from the slope of the regression between Ag influx into *L. stagnalis* and the waterborne Ag exposure concentrations (data from the linear

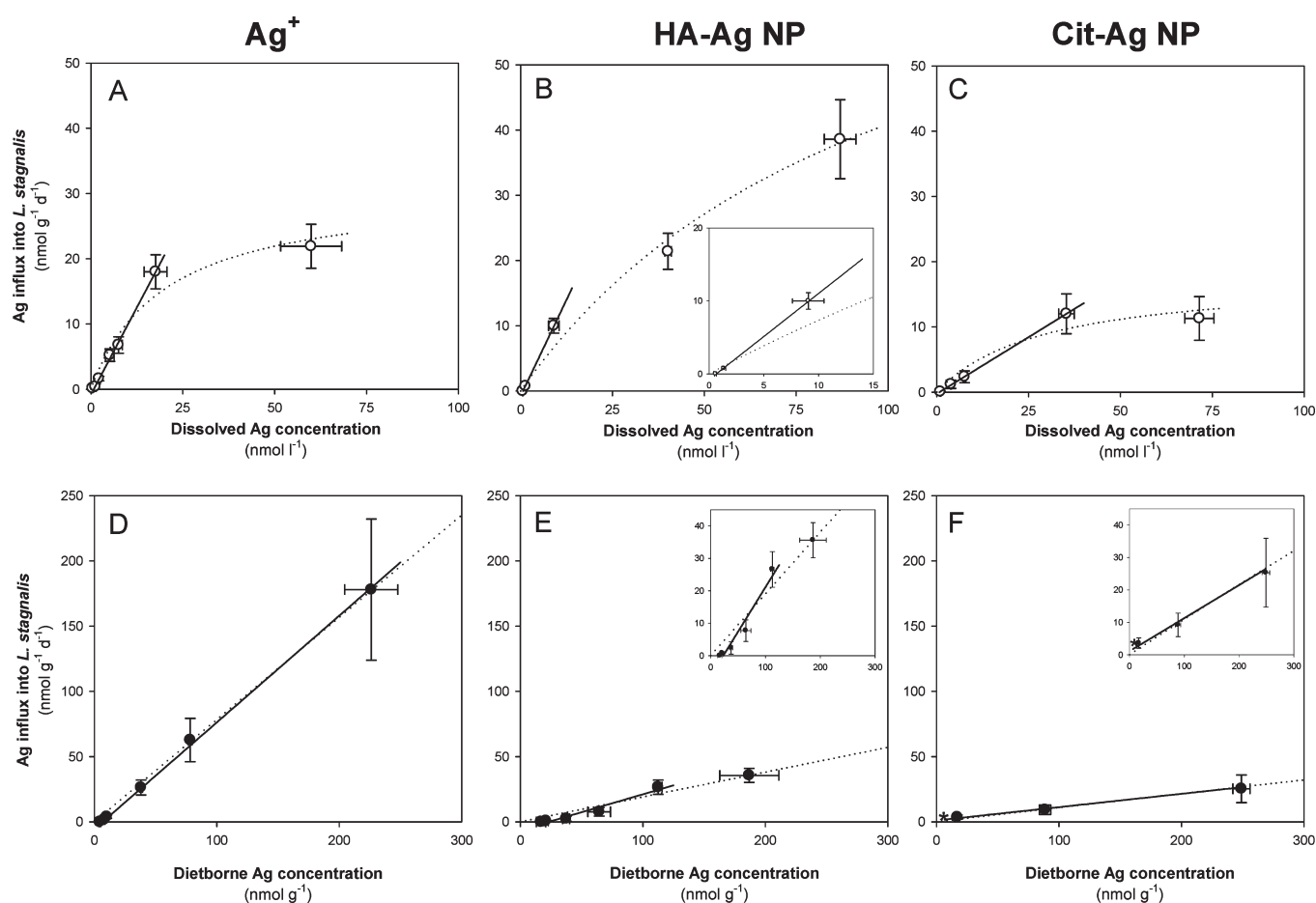


Figure 2. Silver uptake rates ($\text{nmol g}^{-1} \text{d}^{-1} \pm 95\% \text{ C.I.}$) in *L. stagnalis* soft tissue after waterborne and dietborne exposures. Each symbol represents Ag concentrations (from which background Ag was removed) for 10 individuals and 5 water or diatoms samples ($\pm 95\% \text{ C.I.}$). Open circles are for the dissolved exposure; solid circles are for dietary exposures. Solid lines represent linear regression relationships; dotted lines represent nonlinear regression fits to Michaelis–Menten equation (eq 2). Inset in panels B, E, and F shows data at a smaller scale.

portion of the curve), were 1.1 ± 0.1 for Ag^+ , 1.2 ± 0.2 for HA-Ag NPs, and 0.35 ± 0.01 for cit-Ag NPs (Table 1).

Silver influxes from solution demonstrated saturation uptake kinetics for all forms of Ag at high exposure concentrations (Figure 2A–C, dotted lines). The saturation point of the Ag influx curves was lowest for cit-Ag NPs and highest for HA-Ag NPs. Specifically, binding site capacity ($B_{\text{max}} \pm \text{SE}$ in nmol g^{-1}) increases in the order cit-Ag NPs (18 ± 6) < Ag^+ (31 ± 5) < HA-Ag NPs (82 ± 26) (Table 1). The dissolved Ag concentrations at half saturation ($K_{\text{Ag-snail}} \pm \text{SE}$ in nmol l^{-1}) increase in the order Ag^+ (20 ± 7.5) < cit-Ag NPs (36 ± 11) < HA-Ag NPs (101 ± 54).

Silver Uptake from Food. Snails exposed for 2–4 h to dietborne Ag concentrations ranging from 8 to 250 nmol g^{-1} took up detectable Ag when concentrations of Ag in food exceeded ~ 10 and 17 nmol g^{-1} for HA-Ag NPs and cit-Ag NPs, respectively (Figure 2D–F; Figure S5B of the SI). Uptake rates from diet increased linearly over the full range of concentrations for all forms of Ag. The Ag uptake rate constant from food ($k_{\text{uf}} \pm 95\% \text{ C.I.}$ in $\text{g g}^{-1} \text{d}^{-1}$), as determined from the slope of the regression between Ag uptake rate into *L. stagnalis* and the dietborne Ag exposure concentrations (data from the linear portion of the curve), was significantly higher ($p < 0.001$) for Ag^+ (0.81 ± 0.03) than for HA-Ag NPs (0.27 ± 0.12) and cit-Ag

NPs (0.10 ± 0.09) (Table 1). Dietborne Ag influx is thus 3 to 8-times faster when snails fed on diatoms pre-exposed to Ag^+ compared to when fed Ag NPs mixed with diatoms.

The membrane characteristics exceeded the exposure concentrations for each Ag form (Figure 2D–F, dotted lines), and are thus not reported.

Biodynamic Parameters for Ag Uptake. Silver was efficiently assimilated from all forms of Ag. Silver AE ($\% \pm 95\% \text{ C.I.}$) was on average higher for Ag incorporated in diatoms after dissolved exposure to AgNO_3 (73 ± 5) and lower for Ag NPs mixed with diatoms (i.e., 49 ± 7 for HA-Ag NPs and 58 ± 8 for cit-Ag NPs; Table 1; Figure S6A–C of the SI). Food IR was also higher when snails were offered diatoms pre-exposed to Ag^+ than when offered Ag NPs mixed with diatoms. Specifically, snails ingested diatoms pre-exposed to Ag^+ at a rate averaging $0.91 \text{ g g}^{-1} \text{d}^{-1}$, whereas food IR varied (on average) from 0.24 to $0.29 \text{ g g}^{-1} \text{d}^{-1}$ when offered diatoms mixed with Ag NPs (Table 1, Figure S6D–F of the SI). The difference between the Ag^+ and the Ag NPs feeding rates suggests that some avoidance of food occurs whenever there were Ag NPs in the food. Feeding was further inhibited with increasing concentrations of cit-Ag NPs in diet. Specifically, food IR declined from 0.43 to $0.14 \text{ g g}^{-1} \text{d}^{-1}$ when dietborne Ag exposures from cit-Ag NPs varied from 17 to 250 nmol g^{-1} (Figure S6F of the SI).

Table 1. Biodynamic Parameters ($\pm 95\%$ C.I.) and Metal Binding Characteristics (\pm S.E.) for Ag by *L. stagnalis*^a

	Ag ⁺	cit-Ag NPs	HA-Ag NPs
biodynamic parameters			
k_{uw} (l g ⁻¹ d ⁻¹) ^b	1.1 \pm 0.1 (6)	0.35 \pm 0.01 (4)	1.2 \pm 0.2 (3)
k_{uf} (g g ⁻¹ d ⁻¹) ^b	0.81 \pm 0.03 (6)	0.10 \pm 0.09 (3)	0.27 \pm 0.12 (5)
k_{ew} (d ⁻¹) ^b	0.004 \pm 0.013 (9)	0.058 \pm 0.019 (9)	0.051 \pm 0.020 (11)
k_{ef} (d ⁻¹) ^b	0.005 \pm 0.031 (7)	N.D. (7) ^d	0.075 \pm 0.026 (7)
k_{gw} (d ⁻¹) ^c	N.D. (70) ^d	0.008 \pm 0.005 (92)	0.015 \pm 0.003 (110)
k_{gf} (d ⁻¹) ^c	0.036 \pm 0.006 (69)	N.D. (69) ^d	0.031 \pm 0.006 (78)
AE (%) ^c	73 \pm 5 (44)	58 \pm 8 (27)	49 \pm 7 (30)
IR (g g ⁻¹ d ⁻¹) ^c	0.91 \pm 0.09 (44)	0.24 \pm 0.07 (27)	0.29 \pm 0.04 (30)
defecation rate (g g ⁻¹ d ⁻¹) ^c	0.066 \pm 0.005 (64)	0.041 \pm 0.005 (54)	0.052 \pm 0.005 (54)
metal binding characteristics			
B_{max} (nmol g ⁻¹) ^b	31 \pm 5 (7)	18 \pm 6 (5)	82 \pm 26 (5)
K_{metal} (nmol l ⁻¹) ^b	20 \pm 7 (7)	29 \pm 23 (5)	101 \pm 54 (5)

^aN.D. Not detected. ^bThe number of replicate samples containing 10 individual snails is in parentheses. ^cThe number of individual snails is in parentheses. ^dSet at 0.001 for modeling.

Defecation rates during the 48 h period following the pulse exposure were highest for Ag⁺, lowest for cit-Ag NPs and intermediate for HA-Ag NPs (Table 1), consistent with the differences in ingestion rates (Figure S6G-I of the SI). Exposure concentrations did not influence defecation rates ($p > 0.1$). However, SEM images of feces harvested during the depuration phase show a large proportion of undigested diatoms in feces of snails exposed to the highest concentrations of Ag NPs in contrast to very few intact diatoms in feces of snails exposed to the lowest Ag NPs concentrations (Figure 1B–C, Figure S7 of the SI), which supports the suggestion of dietary stress at high Ag NPs concentrations.

Elimination of Accumulated Ag. After being incorporated into tissues from dissolved or dietary sources, Ag⁺ was lost extremely slowly, if lost at all, when the source was removed (Figure 3A,D). The rate constant of physiological loss in these experiments, determined by nonlinear regression using a single exponential loss equation (eq S5 of the SI), was not significantly different than zero (Table 1). In contrast, Ag accumulated after exposure to both Ag NPs in water was lost relatively rapidly ($\sim 5\%$ per day). When exposure was via food, HA-Ag NPs had a similar rate constant of loss as in the waterborne exposure, but cit-Ag NPs were retained with no detectable loss after defecation of the material in the gut (Figure 3).

Snails gained weight significantly during the depuration phase following some of the waterborne or dietborne Ag exposures (Figure S8 of the SI). Growth rate constants (k_g), determined by fitting the dry weight of the experimental organisms to an exponential growth function (eq S6), varied from undetectable to up to 0.036 d⁻¹ during the depuration phase (Table 1). The loss due to growth dilution was subtracted from the observed loss of Ag to determine the physiological rate constant of loss of Ag. Snails did not grow after waterborne exposure to Ag⁺ (Figure S8A of the SI) and after exposure to cit-Ag NPs in diet (Figure S8F of the SI).

DISCUSSION

Silver Uptake from Solution. The characteristics of Ag uptake differed among Ag forms. The rate constant of Ag uptake from water for Ag⁺ is clearly higher than that for cit-Ag NPs, but

the k_{uw} s are comparable between HA-Ag NPs dispersed in water and Ag⁺. It should be kept in mind, however, that these experimentally determined uptake rate constants may be higher than those found in many natural waters which have higher concentrations of agents that might complex Ag and reduce its bioavailability.²⁶ Possible explanations for the greater waterborne uptake of Ag from HA-Ag NPs compared to that from cit-Ag NPs include (i) a greater solubility in MOD water of the HA-Ag NPs than that predicted from the solubility experiment conducted in 0.001 NaNO₃ where <0.05% of the total Ag was released from HA-Ag NPs (no measurable dissolved Ag was released from cit-Ag NPs⁹); (ii) a weaker tendency of the HA-Ag NPs to aggregate compared to the cit-Ag NPs, favoring their waterborne uptake, (iii) greater number of binding sites for HA-NPs making faster influx possible, and/or (iv) stronger binding of HA-Ag NPs compared to the cit-Ag NPs to the snail's surface where they steadily release Ag⁺. A more detailed investigation is necessary to identify the mechanisms behind these differences. But this does support the concept that waterborne Ag uptake from the Ag NPs is more complex than simply dissolution into Ag⁺ (e.g., refs 27 and 28). The differences in loss dynamics further suggest that the form of Ag accumulated by the animals from waterborne Ag NPs was probably not Ag ion.

Silver Uptake from Food and Dietary Metal Stress. All forms of Ag appear highly bioavailable to *L. stagnalis* from diet (AE > 49%). The high Ag AEs are comparable to those observed in a predatory snail,²⁹ but are lower than the Ag AEs observed in marine herbivores (e.g., ref 30). *L. stagnalis* assimilate Ag from Ag NPs mixed with food with a somewhat lower AE than Ag from diatoms pre-exposed to Ag⁺, however. One possibility is that less cytosolic Ag is present in the algal cells exposed to Ag NPs, reducing concentrations of one form of bioavailable Ag in food.³¹

Diatoms pre-exposed to Ag⁺ appear more palatable to snails compared to diatoms mixed with Ag NPs (Figures S6D–F of the SI), which explain in part the higher k_{uf} found for Ag-laden diatoms compared to the k_{uf} for Ag NPs mixed with diatoms. The low IR in snails exposed to Ag NPs did not noticeably enhance AE, as is sometimes observed.³⁰ This implies that what is understood about dietary metal bioavailability from labeling food with dissolved ionic metals might not apply to these Ag NPs particles entrained in food. The ability to assimilate Ag from food

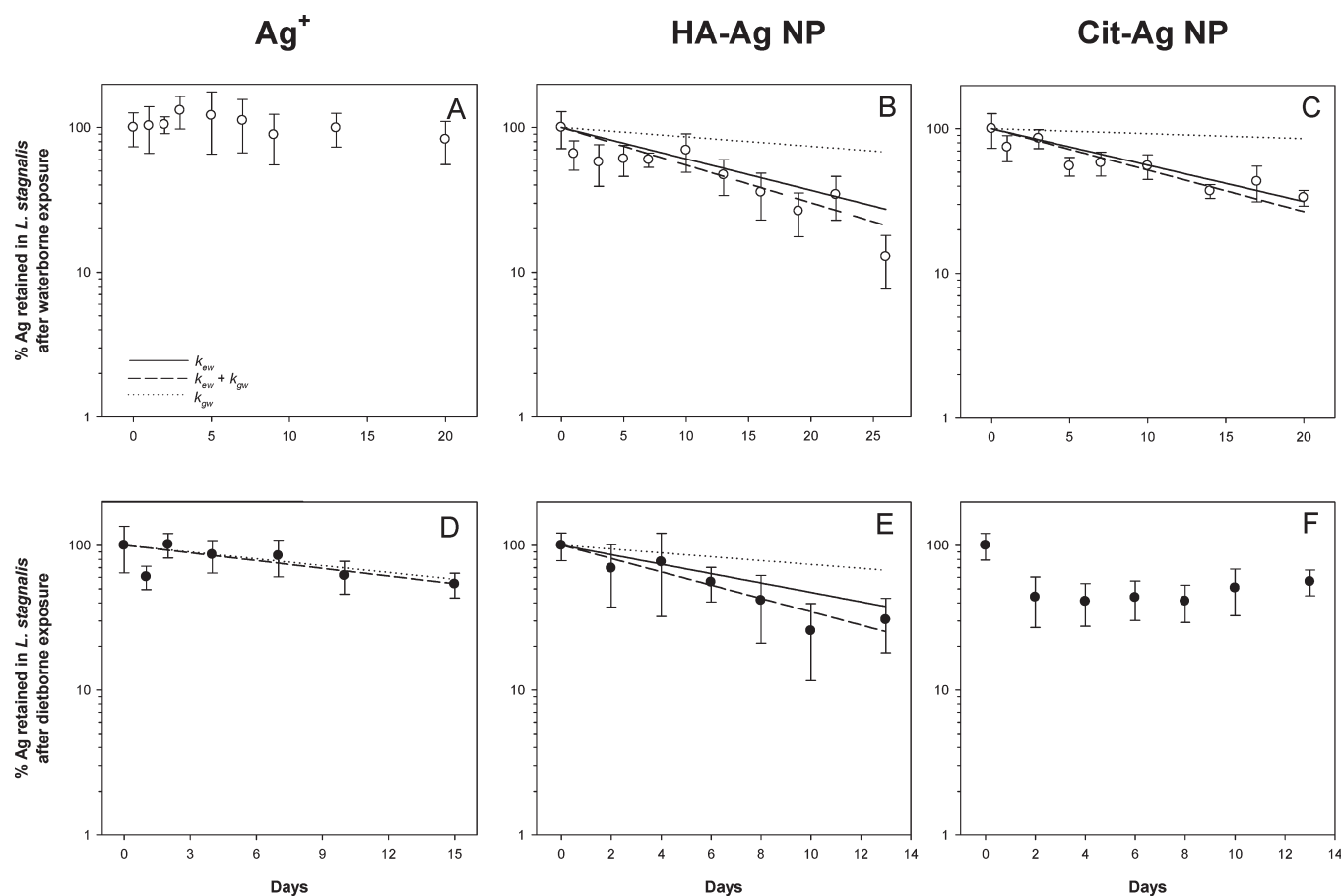


Figure 3. Proportional loss of Ag over time in *L. stagnalis* after waterborne and dietborne exposures. Each symbol represents Ag concentrations (from which background Ag was removed) for 10 individuals ($\pm 95\%$ C.I.). Open circles are for the dissolved exposure; solid circles are for dietary exposures. Solid lines represent net loss of Ag; dotted lines represent body growth dilution; dashed lines represent the combined loss through elimination and growth dilution.

was not impaired by the Ag concentrations, but snails did appear to avoid the Ag NPs in diet, as observed for earthworms exposed to Ag NPs.³² The mechanisms behind such a behavioral response are unclear, however. The further inhibition in feeding observed as cit-Ag NP concentrations rise suggests additional damage or dietary stress when cit-Ag NPs get high in concentration. Accentuation of feeding inhibition at high dietborne concentrations has also been observed for Cu³³ and for ZnO nanoparticles in *L. stagnalis*.²⁴ The chemicals used to synthesize and modify the surface chemistry of cit-Ag NPs (i.e., sodium borohydride and sodium citrate) were not the cause of the inhibited feeding rates (data not shown).

Although the reduced feeding rates on the Ag NPs spiked diatoms carried over to reduced defecation rates, the further inhibition of feeding by cit-Ag NPs at high concentrations was not accompanied by further inhibition of defecation. This suggests a rapid recovery from the latter form of dietary stress when the animals were fed unspiked food for 48 h. In contrast, snails exposed to high concentrations of ZnO nanoparticles in the diet did not show detectable signs of recovery after 48 h of depuration.²⁴ SEM images of feces harvested after the depuration phase (Figure 1 and Figure S7 of the SI) provided evidence of damaged digestion from the high concentrations of cit-Ag NPs, however.

Like bivalves, snails might modify their digestion strategy and process food differently when it contains high concentrations of

contaminants (e.g., Ag NPs). In bivalves, contaminated food is processed through a more rapid intestinal pathway that would probably result in less efficient digestion.³⁴ Whatever the cause, disruption of gut function along with reduced feeding activity can trigger adverse effects that can propagate to higher level processes like growth and reproduction, and ultimately affect populations and communities. Feeding rates, defecation rates, and measurements of assimilation efficiency should thus be examined along with SEM images of feces when assessing dietary metal toxicity.

Predicting Ag Bioavailability, Bioaccumulation and Toxicity. Incorporation of the Ag uptake and loss parameters into the integrated form of eq 1 (eq S1 of the SI) shows that dietary exposure to all forms of Ag, especially the cit-Ag NPs, would result in high Ag body concentrations in *L. stagnalis*. The low rate constants of loss are the primary drivers of this high bioaccumulation (Table 1). For instance, chronic exposure to 50 nmoles g⁻¹ of dietborne Ag in the form of Ag⁺, cit-Ag NPs, and HA-Ag NPs would yield steady-state Ag concentrations of 990, 2500, and 125 nmoles g⁻¹, respectively. If we assume that a waterborne Ag concentration of 0.25 nmoles l⁻¹ would accompany the dietborne concentrations above, then snails would bioaccumulate only 55, 1, and 5 nmoles g⁻¹ of Ag from Ag⁺, cit-Ag NPs, and HA-Ag NPs, respectively. Such a partitioning difference is typical of Ag in the environment, but partitioning of different types of Ag

NPs between water and particulate forms is not yet well-known. Under the assumptions above, diet is the main route of Ag uptake in *L. stagnalis*, as observed for other metals.³³ Given the link between bioaccumulation and toxicity, dietborne exposures to Ag, including Ag NPs, are likely to elicit adverse effects more readily than waterborne exposures.

Proliferation of Ag nanotechnologies is likely to result in Ag concentration in the ng l⁻¹ range in natural waters.¹³ Difficulties in detecting Ag NPs within this range are likely to limit environmental surveillance until new tools (e.g., isotope tracers, analytical instruments) become available to effectively address the environmental risks of this emerging nanotechnology. Equation 1 along with appropriate biodynamic parameters could be used to estimate bioavailable Ag concentrations in nature and overcome some of the difficulties of directly measuring and detecting Ag NPs in the environment.

■ ASSOCIATED CONTENT

S Supporting Information. TEM images and size distribution for cit-Ag NPs and HA-Ag NPs, particle characterization, ionic composition of the MOD water, biodynamic model equations, EDTA extraction procedure, SEM images, and pictures of diatom mats onto which Ag NPs were filtered through, metal analysis using ICP-MS, Ag concentrations in *L. stagnalis* after waterborne and dietborne exposures, Ag AE, food IR, and defecation rates as a function of Ag exposure concentrations, comparative SEM images of feces after dietborne exposures to cit-Ag NPs, and dry weight in *L. stagnalis* as a function of time during depuration (Figures S1–S8). This material is available free of charge via the Internet at <http://pubs.acs.org>.

■ AUTHOR INFORMATION

Corresponding Author

*E-mail: mcroteau@usgs.gov.

■ ACKNOWLEDGMENT

Funding for this work was provided from the Toxic Substances Research Program of the U.S. Geological Survey, the National Research Program (USGS) and by a grant from the Leverhulme Trust (F/00 696/N). The authors thank A. D. Dybowska and D. Berhanu for their assistance with particle synthesis and characterization, D. B. Kent for help with the chemical speciation calculations, J. A. Garcia for his assistance with biodynamics experiments as well as A. Kleckner and D. J. Cain for help with algal cultures. Critical comments from D. J. Cain and A. D. Dybowska are greatly appreciated.

■ REFERENCES

- (1) The Project on Emerging Nanotechnologies. <http://www.nanotechnology.org/>.
- (2) Mueller, N. C.; Nowack, B. Exposure modeling of engineered nanoparticles in the environment. *Environ. Sci. Technol.* **2008**, *42*, 4447–4453.
- (3) Liao, S. Y.; Read, D. C.; Pugh, W. J.; Furr, J. R.; Russel, A. D. Interaction of silver nitrate with readily identifiable groups: relationship to the antibacterial action of silver ions. *Lett. Appl. Microbiol.* **1997**, *25*, 279–283.
- (4) Ratte, H. T. Bioaccumulation and toxicity of silver compounds: A review. *Environ. Toxicol. Chem.* **1999**, *18*, 89–108.

- (5) Lee, K. J.; Nallathamby, P. D.; Browning, L. M.; Osgood, C. J.; Xu, X.-H. N. In vivo imaging of transport and biocompatibility of single silver nanoparticles in early development of zebrafish embryos. *ACS Nano* **2007**, *1*, 133–143.

- (6) Luoma, S. N.; Rainbow, P. S. Why is metal bioaccumulation so variable? Biodynamics as a unifying concept. *Environ. Sci. Technol.* **2005**, *39*, 1921–1931.

- (7) Rainbow, P. S. Trace metal concentrations in aquatic invertebrates: Why and so what? *Environ. Pollut.* **2002**, *120*, 497–507.

- (8) Kittler, S.; Greulich, C.; Diendorf, J.; Köller, M.; Eppe, M. Toxicity of silver nanoparticles increases during storage because of slow dissolution under release if silver ions. *Chem. Mater.* **2010**, *22*, 4548–4554.

- (9) Misra, S. K.; Dybowska, A.; Berhanu, D.; Krisnadason, S.; Croteau, M.-N.; Luoma, S. N.; Boccacini, A. R.; Valsami-Jones, E. Surface modification—The key to dissolution and fate of silver nanoparticles. *Nano Lett.* In preparation.

- (10) Navarro, E.; Piccapietra, F.; Wagner, B.; Marconi, F.; Kaegi, R.; Odzak, N.; Sigg, L.; Behra, R. Toxicity of silver nanoparticles to *Chlamydomonas reinhardtii*. *Environ. Sci. Technol.* **2008**, *42*, 8959–8964.

- (11) Garcia-Alonso, J.; Khan, F. R.; Misra, S. K.; Turmaine, M.; Smith, B. D.; Rainbow, P. S.; Luoma, S. N.; Valsami-Jones, E. Cellular internalization of silver nanoparticles in gut epithelia of the estuarine polychaete *Nereis diversicolor*. *Environ. Sci. Technol.* **2011**, *45*, 4630–4636.

- (12) Liu, J.; Hurt, R. H. Ion release kinetics and particle persistence in aqueous nano-silver colloids. *Environ. Sci. Technol.* **2010**, *44*, 2169–2175.

- (13) Luoma, S. N. Silver nanotechnologies and the environment: Old problems or new challenges. Project on Emerging Nanotechnologies, Publication 15. Washington DC, 2008.

- (14) Bergsma, J.; Konings, W. N. The properties of citrate transport in membrane vesicles from *Bacillus subtilis*. *Eur. J. Biochem.* **1983**, *134*, 151–156.

- (15) Chuang, C.-Y.; Wang, W.-X. Co-transport of metal complexes by the green mussel *Perna viridis*. *Environ. Sci. Technol.* **2006**, *40*, 4523–4527.

- (16) Pärt, P.; Wilmark, G. The influence of some complexing agents (EDTA and citrate) on the uptake of cadmium in perfused rainbow trout gills. *Aquat. Toxicol.* **1984**, *5*, 277–289.

- (17) Roditi, H. A.; Fisher, N. S.; Sañudo-Wilhelmy, S. A. Uptake of dissolved organic carbon and trace elements by zebra mussels. *Nature* **2000**, *407*, 78–80.

- (18) Voets, J.; Bervoets, L.; Blust, R. Cadmium bioavailability and accumulation in the presence of humic acid to the Zebra Mussel, *Dreissena polymorpha*. *Environ. Sci. Technol.* **2004**, *38*, 1003–1008.

- (19) Fabrega, J.; Fawcett, S. R.; Renshaw, J. C.; Lead, J. R. Silver nanoparticle impact on bacterial growth: effect of pH, concentration, and organic matter. *Environ. Sci. Technol.* **2009**, *43*, 7285–7290.

- (20) Parkhurst, D. L.; Appelo, C. A. J. User's guide to PHREEQC (version 2) — A computer program for speciation, batch-reaction, one-dimensional transport, and inverse geochemical calculations. *Water Resour. Invest. Rept.*, 99–4259, Northborough, MA, 1999.

- (21) Wen, L.-S.; Santschi, P. H.; Gill, G. A.; Tang, D. Silver concentrations in Colorado, USA, watersheds using improved methodology. *Environ. Toxicol. Chem.* **2002**, *21*, 2040–2051.

- (22) Irving, E. C.; Baird, D. J.; Culp, J. M. Ecotoxicological responses of the mayfly *Baetis tricaudatus* to dietary and waterborne cadmium: Implications for toxicity testing. *Environ. Toxicol. Chem.* **2003**, *22*, 1058–1064.

- (23) U.S. Environmental Protection Agency: *Methods for Measuring the Acute Toxicity of Effluents and Receiving Waters to Freshwater and Marine Organisms*; U.S. EPA: Washington DC, 2002; EPA-821-R-02–012.

- (24) Croteau, M.-N.; Dybowska, A. D.; Luoma, S. N.; Valsami-Jones, E. A novel approach reveals that zinc oxide nanoparticles are bioavailable and toxic after dietary exposures. *Nanotoxicology* **2011**, *5*, 79–90.

- (25) Croteau, M.-N.; Luoma, S. N.; Pellet, B. Determining metal assimilation efficiency in aquatic invertebrates using enriched stable metal isotope tracers. *Aquat. Toxicol.* **2007**, *83*, 116–125.

- (26) Adams, N. W. H.; Kramer, J. R. Silver speciation in wastewater effluent, surface waters, and pore waters. *Environ. Toxicol. Chem.* **1999**, *18*, 2667–2673.
- (27) Gratton, S. E.; Ropp, P. A.; Pohlhaus, P. D.; Luft, J. C.; Madden, V. J.; Napier, M. E.; DeSimone, J. M. The effect of particle design on cellular internalization pathways. *Proc. Natl. Acad. Sci.* **2008**, *105*, 11613–11618.
- (28) Chithrani, B. D.; Ghazani, A. A.; Chan, W. C. W. Determining the size and shape dependence of gold nanoparticle uptake into mammalian cells. *Nano Lett.* **2006**, *6*, 662–668.
- (29) Cheung, M.; Wang, W.-X. Influence of subcellular metal compartmentalization in different prey on the transfer of metals to a predatory gastropod. *Mar. Ecol.: Prog. Ser.* **2005**, *286*, 155–166.
- (30) Wang, W.-X.; Fisher, N. S.; Luoma, S. N. Assimilation of trace elements ingested by the mussel *Mytilus edulis*: Effects of algal food abundance. *Mar. Ecol.: Prog. Ser.* **1995**, *129*, 165–176.
- (31) Reinfelder, J. R.; Fisher, N. S. The assimilation of elements ingested by marine copepods. *Science* **1991**, *251*, 794–796.
- (32) Shoults-Wilson, W. A.; Zhurbich, O. I.; McNear, D. H.; Tsyusko, O. V.; Bertsch, P.; Unrine, J. M. Evidence for avoidance of Ag nanoparticles by earthworms (*Eisenia fetida*). *Ecotoxicology* **2011**, *20*, 385–396.
- (33) Croteau, M.-N.; Luoma, S. N. Predicting dietborne metal toxicity from metal influxes. *Environ. Sci. Technol.* **2009**, *43*, 4915–4921.
- (34) Decho, A. W.; Luoma, S. N. Flexible digestion strategies and trace metal assimilation in marine bivalves. *Limnol. Oceanogr.* **1996**, *41*, 568–572.